

Modeling the Two-Strain Dynamics of COVID-19 in Ghana Using a Logistic Growth Model

Monica Veronica Crankson¹, John Cobbinah^{1, 2, *}, Samuella Boadi^{1, 2}

¹Department of Mathematical Science, University of Mines and Technology, Tarkwa, Ghana

²Department of Mathematical Sciences, Ball State University, Muncie, USA

Email address:

johncobbinah2017@gmail.com (John Cobbinah), samuellaboadi@gmail.com (Samuella Boadi),

mcrankson@umat.edu.gh (Monica Veronica Crankson)

*Corresponding author

To cite this article:

Monica Veronica Crankson, John Cobbinah, Samuella Boadi. (2024). Modeling the Two-Strain Dynamics of COVID-19 in Ghana Using a Logistic Growth Model. *American Journal of Applied Mathematics*, 12(5), 149-166. <https://doi.org/10.11648/j.ajam.20241205.15>

Received: 28 July 2024; **Accepted:** 16 August 2024; **Published:** 29 September 2024

Abstract: Through mutation, viruses constantly change, bringing into existence new variants; SARS-CoV-2 is no different. In December 2020, variants with different characteristics that could affect transmissibility and death emerged around the world of which Ghana is not an exception. To address this new phenomenon, a two-strain mathematical model of SARS-CoV-2 was formulated to analyze the transmission dynamics in Ghana. The disease-free equilibrium was calculated. The basic reproduction number, $R_0 = \max\{R_{0A}, R_{0B}\} = \max(0.9957945674, 1.109170840)$, associated with the model is computed using the next generation matrix operator. The disease-free equilibrium is found to be locally asymptotically stable when both $R_{0A}, R_{0B} < 1$, but unstable otherwise. In addition to the disease-free, the boundary equilibrium for strain A and strain B was also calculated. Using the Gersgorin's circle theorem, it was shown that the boundary equilibrium is locally asymptotically stable when both $R_{0A}, R_{0B} > 1$, but unstable when otherwise. Simulations of the model were carried out. Results indicate that the government should intensify its efforts to vaccinate a larger proportion of the population and also recommends implementing comprehensive control measures, such as the use of face masks, social distancing, and contact tracing, to mitigate the spread of the disease.

Keywords: COVID-19, SARS-CoV-2, SVEIR Transmission Dynamics, Diseases-free Equilibrium, Boundary Equilibrium, Stability Analysis, Simulation

1. Introduction

The severe acute respiratory syndrome coronavirus 2 (SARS-CoV-2) also known as COVID-19 is believed to have emerged in Wuhan, China in late 2019 [1]. COVID-19 is an infectious disease that has targeted many people and it is spreading rapidly around the world, causing serious loss of life and potential long-term economic consequences. In January 2020, COVID-19 was declared a public health emergency of international concern and a pandemic in March 2020 [2]

According to the World Health Organisation, there has been 196,553,009 confirmed cases globally of which 4,200,412 have died as of 30th July, 2021 [3]. From this statistic, Covid-19 is considered as one of the deadliest pandemics in history. Ghana experienced a sharp increase in the number of confirmed cases of the COVID-19 as a result of the evasion

of the multiple variants by travellers who entered the country in January 2021. According to the World Health Organisation, as of 30th July 2021, the number of confirmed cases in Ghana since the outbreak stood at 103,019 of which 824 people were reported to have died [4]. An increase in the number of cases has put more strain on health care resources, leading to more hospitalisations, and potentially more deaths in the country.

Generally, viruses constantly change through mutation, and new variants of a virus are expected to occur over time. The deadly COVID-19 virus has undergone a series of mutations as it passed from person to person. However, multiple variants of the virus that causes COVID-19 are circulating globally [5]. The United Kingdom (UK) identified a more easily and quickly spread variant called B.1.1.7 (Alpha) with a large

number of mutations accounting for about 86 percent of infections, than in November to December 2020 when it was just 16 percent. In South Africa, another variant called B.1.351 (Beta) emerged independently of B.1.1.7. Originally detected in early October 2020, B.1.351 shares some mutations with B.1.1.7. In Brazil, a variant called P.1 (Gamma) emerged that was first identified in travellers from Brazil, who were tested during routine screening at an airport in Japan, in early January [6]. This variant contains a set of additional mutations that may affect its ability to be recognised by antibodies. A new variant has emerged called B.1.617.2 (Delta). This variant was first detected in the United States in March 2021 which was initially identified in India in December 2020 [7]. These variants seem to spread more easily and quickly than other variants, which may lead to more cases of COVID-19. An increase in the number of cases will put more strain on healthcare resources, lead to more hospitalizations, and potentially more deaths [8].

Epidemiological studies have shown that mutations have led to more and more drug-resistant viruses giving the appearance of many new harmful epidemics or even new dangerous pandemics [9]. According to the Centers for Disease Control and Prevention (CDC), the reappearance of infectious diseases is due to the presence of unvaccinated individuals and their interaction with other people who have contracted the disease from other countries [10].

Although, the reinfection of COVID-19 and multiple viral strains have become the subject of many literatures, mathematical models that incorporate these characteristics are still lacking [11]. However, among the novel contributions made towards multiple strain COVID-19 modeling, this research considers two viral strains of COVID-19 in Ghana with logistic growth model.

2. Methods

This section outlines the methods and mathematical concepts employed to obtain the results of this research. It covers various topics, including differential equations, compartmental models, the Jacobian matrix, the basic reproduction number and its calculation using the next-generation matrix.

2.1. Differential Equation

A differential equation is an equation that relates one or more function and their derivatives [12]. In applications, the functions generally represent physical quantities, the derivatives describe their rates of change, and the differential equation describes the relationship between the two. A solution to a differential equation is a function $y = f(x_1, x_2, \dots, x_n)$ that satisfies the differential equation when f and its derivatives are substituted into the equation.

Differential equations first brought into existence by the invention of calculus by Newton and Leibniz. Isaac Newton,

in his 1671 work, listed three kinds of differential equations:

$$\begin{cases} \frac{dy}{dx} = f(x) \\ \frac{dy}{dx} = f(x, y) \\ x_1 \frac{\partial y}{\partial x_1} + x_2 \frac{\partial y}{\partial x_2} = y \end{cases} \quad (1)$$

where in all these cases, is an unknown function of x (x_1 and x_2) and f is a given function. He solved these examples and others by using infinite series and discussed the non-uniqueness of solutions. The following are some other examples of differential equations involving the unknown function

$$\begin{cases} \frac{dy}{dx} = 5x + 3 \\ e^y \frac{d^2y}{dx^2} + (\sin x) \frac{d^2y}{dx^2} + 5xy = 0 \\ (4 \frac{d^2y}{dx^2})^3 + 3y(\frac{dy}{dx})^7 + y^3(\frac{dy}{dx})^2 = 5x \\ \frac{\partial^2 y}{\partial t^2} - 4 \frac{\partial y}{\partial x^2} = 0 \\ \frac{\partial^3 u}{\partial x^2 \partial t} = 1 + \frac{\partial u}{\partial t} \\ a^2 \frac{\partial^2 u}{\partial x^2} = \frac{\partial u}{\partial t} \end{cases} \quad (2)$$

Differential equations can be categorized into several types based on their characteristics: ordinary or partial, linear or nonlinear, and homogeneous or heterogeneous.

Non-linear differential equations are equations where the unknown functions appear either as variables in a polynomial of degree higher than one or within a function that is not a first-degree polynomial. In other words, in a non-linear system of equations, the equations cannot be expressed as linear combinations of the unknown variables or functions. Examples of non-linear equations include:

$$\begin{aligned} \frac{du}{dx} &= u^2 + 4 \text{ (Non-Linear due to } u^2) \\ L \frac{d^2u}{dx^2} + g \sin u &= 0 \text{ (Non-Linear due to the } \sin u) \\ \frac{\partial u}{\partial t} &= 6u \frac{\partial u}{\partial x} - \frac{\partial^3 u}{\partial x^3} \text{ (Non-Linear since the dependent} \\ &\text{variable is multiplying it's derivative)} \end{aligned}$$

A system of non-linear equations consists of two or more equations involving two or more variables, with at least one of the equations being non-linear. An n^{th} order system of continuous differential equations can be represented as follows:

$$\begin{cases} \dot{x}_1(t) = f_1(x_1(t), x_2(t), x_3(t), \dots, x_n(t)) \\ \dot{x}_2 = f_2(x_1(t), x_2(t), x_3(t), \dots, x_n(t)) \\ \vdots \\ \dot{x}_n = f_n(x_1(t), x_2(t), x_3(t), \dots, x_n(t)) \end{cases} \quad (3)$$

which can be expressed in matrix form as

$$\dot{X} = f(x(t), t) \quad (4)$$

where $X = [x_1, x_2, x_3, \dots, x_n]^T$ and $f = [f_1, f_2, f_3, \dots, f_n]^T$

In general, detailed solutions, whether numerical or analytical, are often not the primary focus. Instead, the

emphasis is on characterizing specific aspects of system behavior. For example, the presence and stability of equilibrium points might be examined. In nonlinear systems, additional features such as threshold effects are also considered. The overall approach involves broadly characterizing the critical aspects of the system's behavior.

Equilibrium points

A vector \bar{X} is an equilibrium point for a dynamical system if, once the state vector is equal to \bar{X} , it remains equal to \bar{X} for all future time. Thus:

If $\dot{X} = f(X(t), t)$, then an equilibrium point is a state where \bar{X} satisfies $f(\bar{X}, t) = 0$ for all time t . A system may have none, one, or any number of equilibrium points in virtually any spatial pattern in the state space.

Stability

Suppose \bar{X} is an equilibrium point of a time-invariant system i.e. \bar{X} is an equilibrium point of $\dot{X} = f(x(t), t)$. For a correct definition of stability, it is useful to introduce the notation $S(\bar{X}, R)$ to signify a spherical region in the state space with centre at \bar{X} and radius R .

2.2. Compartmental Model

A compartmental model simplifies the mathematical modeling of infectious diseases by dividing the population into compartments, each representing a different disease status. Common labels for these compartments include S (Susceptible), I (Infectious), D (Deceased), E (Exposed), and R (Recovered). The flow of individuals between these compartments follows a defined order, such as in the $SEIR$ model, which consists of the susceptible, exposed, infectious, and recovered classes, or the $SVEIR$ model, which includes vaccinated individuals as a separate compartment. In these models, individuals within a closed population are categorized into mutually exclusive groups based on their disease status [13]. Each person is in one compartment at a given time but can transition between compartments according to the model's parameters.

2.2.1. The SI Model

The simplest form of disease models is the SI (Susceptible, Infected) model. This model divides the population into two groups: susceptible individuals who can contract the disease and infected individuals who can spread the disease to those in the susceptible group. When a susceptible individual becomes infected, a transition occurs at a rate denoted by β which increases the number of infected individuals while decreasing the number of susceptibles. The SI model assumes that each person in the susceptible population has an equal likelihood of becoming infected through contact with an infected individual. Once infected, individuals remain in the infected state indefinitely, continuing to be infectious for the rest of their lives. This model effectively describes the behavior of diseases such as cytomegalovirus (CMV) or herpes (HSV-1 or HSV-2), which are caused by the Herpesviridae virus.

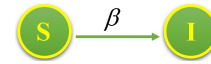


Figure 1. Flow Chart of SI Model.

In the model above, it is assumed that the length of the disease outbreak is short compared with the average person's lifespan, so death and birth are not factors considered. The above model can be formulated as:

$$\begin{cases} \frac{dS}{dt} = -\frac{\beta SI}{N} \\ \frac{dI}{dt} = \frac{\beta SI}{N} \end{cases} \quad (5)$$

where $N = S + I$ is the total population.

2.2.2. The SIR Model

The SIR model is one of the simplest compartmental models, named for its three compartments: Susceptible, Infected, and Recovered. In this model, it is assumed that a susceptible individual can become infected through contact with an infected person [13]. The infected person is assumed to be contagious and can transmit the disease to others. Eventually, the infected individual progresses to a noncontagious state, termed recovery, which may include death or effective isolation.

The recovered class consists of individuals who have been infected and have either recovered from the disease, entered the removed compartment, or died. This model is reasonably predictive for infectious diseases that are transmitted from human to human and where recovery confers lasting immunity, such as measles, mumps, and rubella.

The basic structure of the model (SIR Model), where we do not consider any birth/death process, can be designed as follows:



Figure 2. Flow Chart of SIR Model.

So we have a group of susceptible people who can be infected and get sick with a transmission rate β . Once infected, individuals can get well with a recovery rate of γ . The sum of the three compartments (susceptible, infected and recovered individuals) gives the total population:

$$S + I + R = N \quad (6)$$

We can describe the dynamics of the disease by setting up a system of differential equations, which returns, for each compartment at each point in time, the number of people in that compartment:

$$\begin{cases} \frac{dS}{dt} = -\frac{\beta IS}{N} \\ \frac{dI}{dt} = \frac{\beta IS}{N} - \gamma I \\ \frac{dR}{dt} = \gamma I \end{cases} \quad (7)$$

where the initial conditions are $S(0) = S_0, I(0) = I_0, R(0) = R_0$. Since the total population in this system is conserved, at

any instant if time $S(0) + I(0) + R(0) = S_0 + I_0 + R_0 = \text{constant}$

2.2.3. The SEIR Model

With the *SEIR* model, the total population is divided into four epidemiological classes: Susceptible (*S*), Exposed (*E*), Infectious (*I*), and Recovered (*R*). In this type of model, a prolonged incubation period (the "exposed" category) is experienced, during which infection has occurred but the individual is not yet infectious. For example, diseases like chickenpox and vector-borne illnesses such as dengue hemorrhagic fever have long incubation periods during which transmission of the pathogen to others is not possible. This delay between acquiring the infection and becoming infectious can be integrated into the *SIR* model by introducing a latent/exposed compartment, *E*, and allowing the transition from *S* to *E* and subsequently from *E* to *I*.

The *SEIR* diagram below illustrates how individuals transition through each compartment in the model.

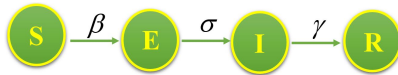


Figure 3. Flow Chart of SEIR Model.

where β is the infection rate, σ is rate at which an infected individual becomes infectious per unit time and γ is the rate at which an infectious individual recovers per unit time. A closed population with no births or deaths has *SEIR* model of the form:

$$\begin{cases} \frac{dS}{dt} = -\frac{\beta SI}{N} \\ \frac{dE}{dt} = \frac{\beta SI}{N} - \sigma E \\ \frac{dI}{dt} = \sigma E - \gamma I \\ \frac{dR}{dt} = \gamma I \end{cases} \quad (8)$$

Where $N = S + E + I + R$ is the total population. Since the latency delays the start of the person's infectious period, the secondary spread from an infected individual will occur later compared with a *SIR* model, where there is no latency. Therefore, including a more extended latency period will result in slow initial growth of the outbreak. But, since the model does not include death population, the basic reproductive number, $R_0 = \frac{\beta}{\gamma}$

2.3. Jacobian Matrix

A Jacobian Matrix can be defined as a matrix that contains a first-order partial derivative for a vector function.

Given a set $y = f(x)$ of n variables $x_1, x_2, x_3, \dots, x_n$ written explicitly as

$$y = \begin{bmatrix} f_1(x) \\ f_2(x) \\ \vdots \\ f_n(x) \end{bmatrix},$$

or more explicitly as

$$\begin{cases} y_1 = f_1(x_1, \dots, x_n) \\ \vdots \\ y_n = f_n(x_1, \dots, x_n) \end{cases} \quad (9)$$

Then Jacobian matrix of y is an $m \times n$ defined as:

$$J(x_1, x_2, x_3, \dots, x_n) = \begin{pmatrix} \frac{\partial y_1}{\partial x_1} & \dots & \frac{\partial y_1}{\partial x_n} \\ \vdots & \ddots & \vdots \\ \frac{\partial y_n}{\partial x_1} & \dots & \frac{\partial y_n}{\partial x_n} \end{pmatrix} \quad (10)$$

The determinant of is the Jacobian and is denoted by

$$J = \left| \frac{\partial(y_1, \dots, y_n)}{\partial(x_1, \dots, x_n)} \right| \quad (11)$$

Consider the example below:

$$\begin{cases} \frac{dx}{dt} = 4x^3 + 3y^2x = f_1 \\ \frac{dy}{dt} = 5y^2 - 2xy + 1 = f_2 \end{cases} \quad (12)$$

From the system of differential equation (12), the Jacobian matrix will be:

$$J_f(x, y) = \begin{pmatrix} \frac{\partial f_1}{\partial x} & \frac{\partial f_1}{\partial y} \\ \frac{\partial f_2}{\partial x} & \frac{\partial f_2}{\partial y} \end{pmatrix} = \begin{pmatrix} 12x^2 + 3y^2 & 6xy \\ -2y & 10y - 2x \end{pmatrix} \quad (13)$$

The Jacobian Matrix is used in the linearisation of non-linear systems around a given equilibrium point. Thus, it allows the use of linear systems techniques, such as calculating eigenvalues (and thus allowing an indication of the type of the equilibrium point).

2.4. Basic Reproduction Number, R_0

The basic reproduction number, R_0 , also known as the basic reproduction ratio, is an epidemiologic metric used to describe the contagiousness or transmissibility of an infectious agent [15]. It is defined as the average number of secondary infections produced by a typical case of a disease in a population where everyone is susceptible. For example, if the R_0 for measles in a population is 2, then one infected person is expected to infect, on average, two new people, assuming everyone around the case is susceptible [16]. It is important to note that R_0 does not include new cases produced by secondary infections.

For an epidemic to occur in a susceptible population, R_0 must be greater than one, meaning the number of cases will increase. In commonly used epidemic models, when $R_0 > 1$, the infection will spread in the population. Conversely, if $R_0 < 1$, the disease will eventually die out. Generally, the higher the R_0 value, the more challenging it is to control the epidemic.

The next-generation matrix in epidemiology is used to determine the basic reproduction number for a compartmental

model of infectious disease spread. It is employed to calculate the basic reproduction number for structured population models in population dynamics [17]. Below is an explanation of how the next-generation matrix can be used to find R_0 :

Let X_S be the set of all disease Free states, that is

$$X_S = \{x \geq 0 | x_i = 0, i = 1, 2, \dots, m\}. \quad (14)$$

In order to compute for R_0 , it is important to distinguish new infections from all other changes in the population.

Let $F_i(x)$ be the rate of appearance of new infections in compartments i

V_i^+ be the rate of transfer of individuals into compartment i by all other means.

V_i^- be the rate of transfer of individuals out of compartment i .

It is assumed that each function ($F_i(x)$, V_i^+ and V_i^-) is continuously differentiable at least twice with respect to each variable. The transmission model consists of the non-negative initial conditions together with the following system of equations.

$$\dot{x} = f_i(x) = F_i(x) - V_i(x), \quad i = 1, 2, 3, \dots, n \quad (15)$$

where $V_i = V_i^- - V_i^+$ and the functions satisfying the following conditions:

C1 : if $x \geq 0$ then $F_i, V_i^-, V_i^+ \geq 0$ for $i = 1, 2, \dots, n$.
If the compartment is empty, then there can be no transfer of individuals out of the compartment by death, infection nor any other means.

C2 : If $x_i \geq 0$ then $V_i^- \geq 0$ (Nobody leaves the compartment). In particular if $x \in X_S$, then $V_i^- = 0$ for $i = 1, 2, \dots, m$.

C3 : $F_i = 0, i > m$ (m is the number of infective classes)

C4 : If $x \in X_S$ then $F_i = 0$, and $V_i = 0$ for $i = 1, 2, \dots, m$.

C5 : If $F(x)$ is set to zero, then all the eigenvalues of $Df(x_0)$ have negative real parts.

Lemma: If x_0 is a disease-free equilibrium (DFE) and $f_i(x)$ satisfies C1 – C5, then the derivatives $DF(x_0)$ and $DV(x_0)$ are partitioned as

$$Df(x_0) = \begin{pmatrix} F & 0 \\ 0 & 0 \end{pmatrix}, \quad DV(x_0) = \begin{pmatrix} V & 0 \\ J_3 & J_4 \end{pmatrix} \quad (16)$$

where F and V are the $m \times m$ matrices defined by

$$F = \left[\frac{\partial F(x_0)}{\partial x_j} \right] \quad \text{and} \quad V = \left[\frac{\partial V(x_0)}{\partial x_j} \right] \quad (17)$$

$$F = \begin{pmatrix} 0 & \beta_1 \\ 0 & 0 \end{pmatrix} \quad \text{and} \quad V = \begin{pmatrix} d+v+r_1 & -pr_2 \\ -v & d+r_2 \end{pmatrix} \quad (23)$$

respectively. The inverse of V is given by

$$V^{-1} = \frac{1}{(d+v+r_1)(d+r_2) - vpr_2} \begin{pmatrix} d+r_2 & pr_2 \\ v & d+v+r_1 \end{pmatrix} \quad (24)$$

with $1 \leq i \leq m$, F is non-negative and V is a non-singular M -matrix

Following Diekmann et al., (1990) [18] we call FV^{-1} the next generation matrix for the model and we shall set R_0 as equal to the spectral radius $\rho(FV^{-1})$ that is:

$$R_0 = \rho(FV^{-1}) \quad (18)$$

Where $\rho(A)$ denotes the spectral of the matrix A

Example 1

Consider the Tuberculosis (TB) treatment model below:

$$\begin{cases} \frac{dS}{dt} = bN - dS - \beta_1 \frac{SI}{N} \\ \frac{dE}{dt} = \beta_1 \frac{SI}{N} + \beta_2 \frac{TI}{N} - d(d+v+r_1)E + pr_2I \\ \frac{dI}{dt} = vE - (d+r_2)I - qr_2I \\ \frac{dT}{dt} = r_1E + qr_2I - dT - \beta_2 \frac{TI}{N} \end{cases} \quad (19)$$

Re-arranging the equations so that we start with infective classes, we obtain

$$\begin{cases} \frac{dE}{dt} = \beta_1 \frac{SI}{N} + \beta_2 \frac{TI}{N} - d(d+v+r_1)E + pr_2I \\ \frac{dI}{dt} = vE - (d+r_2)I - qr_2I \\ \frac{dS}{dt} = bN - dS - \beta_1 \frac{SI}{N} \\ \frac{dT}{dt} = r_1E + qr_2I - dT - \beta_2 \frac{TI}{N} \end{cases} \quad (20)$$

In this case $m = 2$ (Two infected compartments). From (20), we obtain

$$F = \begin{pmatrix} \beta_1 \frac{SI}{N} + \beta_2 \frac{TI}{N} \\ 0 \\ 0 \\ 0 \end{pmatrix} \quad (21)$$

The disease free equilibrium point of the system (21) has coordinates

$$(E^*, I^*, S^*, T^*) = (0, 0, 1, 0) \quad (22)$$

The derivatives of F and V at $(0,0,1,0)$ are given by

and a calculation of gives the reproduction number of the model as

$$R_0 = \frac{v\beta_1}{(d+v+r_1)(d+r_2)-vpr_2} \quad (25)$$

2.5. Logistic Growth Model

A biological population with abundant food, space, and no predator threats grows at a rate proportional to its size. During each time interval, a certain percentage of the individuals reproduce. When reproduction occurs continuously, this growth is described by:

$$\frac{dP}{dt} = rP \quad (26)$$

where P represents the population as a function of time t , and r is the growth rate constant.

However, resource limitations constrain populations in the short term, and no population can grow without limits indefinitely. The figure below shows both logistic and exponential growth patterns. The green curve represents exponential (unconstrained) growth, while the blue curve illustrates logistic growth, constrained by a carrying capacity K . When the population is small compared to K , the two growth patterns are nearly identical, meaning the constraint has little effect. As P becomes a significant fraction of K , the growth patterns begin to diverge. When P approaches K , the growth rate slows and eventually stops. The logistic model is of the form,

$$\frac{dP}{dt} = rP\left(1 - \frac{P}{K}\right) \quad (27)$$

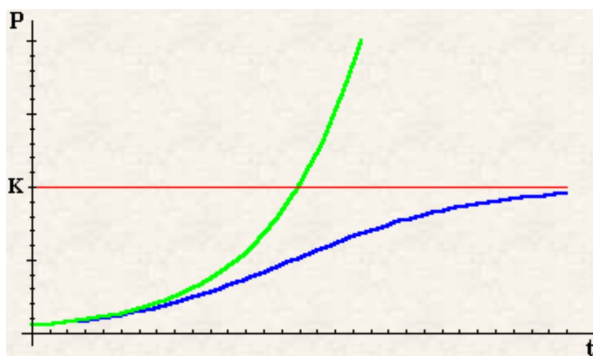


Figure 4. Logistic and exponential growth model.

The logistic model is also known as Verhulst model

3. Model Formulation and Analysis

SARS-CoV-2, through mutation, has undergone some changes, bringing into existence new variants [19]. Recently, a diversification of SARS-CoV-2 due to evolution and adaptation has been observed globally and even in Ghana, but this model considers only two strains (say A and B). Let strain A represent the UK B.1.1.7 strain (also referred to as

Alpha strain) and strain B represent the South Africa (1.351) strain (also referred to as Beta strain) [6].

In this model, only human-to-human transmission of COVID-19 is considered. According to individual's diseases status, the human population at time t denoted by $N(t)$ is divided into sub-populations of susceptible individuals $S(t)$, vaccinated individuals $V(t)$, individuals exposed to strain A $E_1(t)$, individuals exposed to strain B $E_2(t)$, individuals infected with strain A $I_1(t)$, individuals infected with strain B $I_2(t)$ and recovered individuals $R(t)$. The total human population $N(t)$ is given by

$$N(t) = S(t) + V(t) + E_1(t) + E_2(t) + I_1(t) + I_2(t) + R(t) \quad (28)$$

We proposed a model with $bS(1 - \frac{S}{K})$ being the recruitment into the susceptible class (which implies that the susceptible population grows logistically) and assumes a constant natural death rate of μ for all the classes. The susceptible individuals are vaccinated at a rate of ν . The population becomes exposed to strain A at a rate β and strain B at a rate α . The individuals in the exposed classes become infectious at a rate ρ and η for strain A and B , respectively. Infected individuals from strain A (I_1) recover at a rate of τ and have a constant disease-induced death rate of δ , while infected individuals from strain B (I_2) recover at a rate of ϵ and have a constant disease-induced death rate of γ . The model assumes that the disease does not give permanent immunity, but a temporarily acquired immunity and hence recovered individual becomes susceptible again at a rate ω .

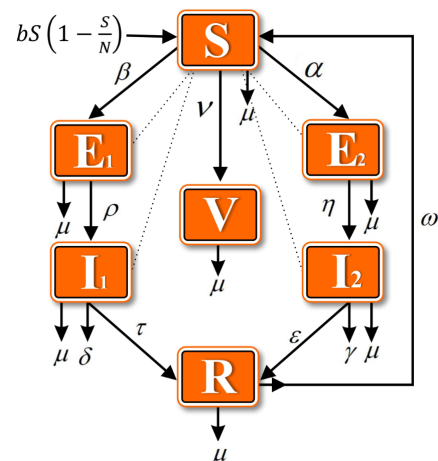


Figure 5. Compartmental Model of the two Strains of SAR-CoV-2.

From the conceptual model flow diagram above, we derive the following deterministic system of nonlinear differential equations

$$\begin{cases} \frac{dS}{dt} = bS \left(1 - \frac{S}{N}\right) - \frac{\beta S(E_1 + \kappa I_1)}{N} - \frac{\alpha S(E_2 + \psi I_2)}{N} - \mu S + \omega R - \nu S \\ \frac{dV}{dt} = \nu S - \mu V \\ \frac{dE_1}{dt} = \frac{\beta S(E_1 + \kappa I_1)}{N} - \rho E_1 - \mu E_1 \\ \frac{dE_2}{dt} = \frac{\alpha S(E_2 + \psi I_2)}{N} - \eta E_2 - \mu E_2 \\ \frac{dI_1}{dt} = \rho E_1 - \tau I_1 - \mu I_1 - \delta I_1 \\ \frac{dI_2}{dt} = \eta E_2 - \epsilon I_2 - \mu I_2 - \gamma I_2 \\ \frac{dR}{dt} = \tau I_1 + \epsilon I_2 - \mu R - \omega R \end{cases} \quad (29)$$

The model assumes that the susceptible population can be infected through contact with the exposed population and the infectious population. However, the model assumes that the rate of infection by the exposed class and infectious class are different, hence the introduction of κ and ψ .

The tables 1 and 3 below describe the variables and parameters that were used in the model above.

Table 1. Model Variables and Definitions.

Variables	Definitions
S	Susceptible Population
V	Vaccinated Population
E_1	Population exposed to Strain A
E_2	Population exposed to Strain B
I_1	Those infectious with Strain A
I_2	Those infectious with Strain B
R	Recovered Population

Table 2. Model Parameter and Definitions.

Parameters	Definitions
b	Recruitment rate into the population
ν	vaccination rate
μ	Natural death rate
β	Rate of infection by strain A
α	Rate of infection by strain B
ρ	Exposure-to-infectious rate for strain A
η	Exposure-to-infectious rate for strain B
τ	Recovery rate of strain A infected individuals
δ	Strain A disease-induced death rate
ϵ	Recovery rate of strain B infected individuals
γ	Strain B disease-induced death rate
ω	Rate of loss of immunity

3.1. Model Assumptions

1. It is assumed that susceptible individual may be exposed to only two strains of the SAR-Cov-2 (Strain A and Strain B)
2. The population is heterogeneous, thus the population is well mixed and the disease can infect both males and female.
3. The model assumes recruitment rate of b into the susceptible class which grows logistically and assumes a constant natural death rate of μ in each of the classes.
4. The model assumes different infection rate for Strain A and Strain B
5. The model assumes that the diseases do not give permanent immunity and hence recovered individual becomes susceptible again at a rate ω .

3.2. Positivity of the Solution

It is assumed from the model that all the variables and the parameters are positive. The initial conditions of the model (29) is defined as:

$S(0) > 0$, $V(0) > 0$, $E_1(0) > 0$, $E_2(0) > 0$, $I_1(0) > 0$, $I_2(0) > 0$, and $R(0) > 0$

Theorem 3.1. Given that $S(0) > 0$, $V(0) > 0$, $E_1(0) > 0$, $E_2(0) > 0$, $I_1(0) > 0$, $I_2(0) > 0$ and $R(0) > 0$, the solution $S(t)$, $E_1(t)$, $E_2(t)$, $I_1(t)$, $I_2(t)$ and $R(t)$ on the model are positively invariant for all $t > 0$.

Proof

In order to prove the positivity result, we let $T = \sup\{\lambda \geq 0 \mid \forall t \in [0, \lambda]\}$ such that $S(t) > 0$, $V(t) > 0$, $E_1(t) > 0$, $E_2(t) > 0$, $I_1(t) > 0$, $I_2(t) > 0$, $R(t) > 0$, then considering the first equation of model (29), we have

$$\frac{dS}{dt} = bS \left(1 - \frac{S}{N}\right) - \frac{\beta(E_1 + \kappa I_1)}{N} S - \frac{\alpha(E_2 + \psi I_2)}{N} S - \mu S - \nu S + \omega R$$

By setting $\theta = \frac{\beta(E_1 + \kappa I_1)}{N} \geq 0$, $\Lambda = \frac{\alpha(E_2 + \psi I_2)}{N} \geq 0$ and $\Pi = bS \left(1 - \frac{S}{N}\right)$, the equation above becomes

$$\frac{dS}{dt} = \Pi - \theta S - \Lambda S - \mu S - \nu S + \omega R \quad (30)$$

Suppose that the solution exists of system (29) for a certain interval $J \in [0, +\infty]$, then the above equation can be solved, for all $t \in J$, as

$$\frac{dS}{dt} + (\theta + \Lambda + \nu + \mu)S = \Pi + \omega R \quad (31)$$

Equation 31 can be solved using the method of integrating factor, so solving for the integration factor (IF), we get

$$IF = e^{\int(\theta+\Lambda+\nu+\mu)dt} = e^{(\mu+\nu)t+\int_0^t(\theta(s)+\Lambda(s))ds} \quad (32)$$

Multiplying equation (31) by the integrating factor (32) and simplifying

$$\frac{d}{dt} \left(S(t)e^{(\mu+\nu)t+\int_0^t(\theta(s)+\Lambda(s))ds} \right) \geq (\Pi + \omega R) \times e^{(\mu+\nu)t+\int_0^t(\theta(s)+\Lambda(s))ds} \quad (33)$$

Taking integral of both sides, we have

$$S(t)e^{(\mu+\nu)t+\int_0^t(\theta(s)+\Lambda(s))ds} - S(0) \geq \int_0^t (\Pi + \omega R) \times e^{(\mu+\nu)u+\int_0^u(\theta(s)+\Lambda(s))ds} du \quad (34)$$

$$S(t)e^{(\mu+\nu)t+\int_0^t(\theta(s)+\Lambda(s))ds} \geq S(0) + \int_0^t (\Pi + \omega R) \times e^{(\mu+\nu)u+\int_0^u(\theta(s)+\Lambda(s))ds} du \quad (35)$$

$$S(t) \geq S(0)e^{-(\mu+\nu)t-\int_0^t(\theta(s)+\Lambda(s))ds} + e^{-(\mu+\nu)t-\int_0^t(\theta(s)+\psi(s))ds} \times \int_0^t (\Pi + \omega R) e^{(\mu+\nu)u+\int_0^u(\theta(s)+\Lambda(s))ds} du > 0 \quad (36)$$

Hence, $\forall t \in \lambda$, $S(t)$ is positive

Now the second equation of the model (29) implicitly shows

$$\frac{dV}{dt} = \nu S - \mu V \geq -\mu V \quad \text{or} \quad \frac{dV}{dt} \geq -\mu V \quad (37)$$

which can be written as

$$\frac{dV}{V} \geq -\mu dt, \quad V \neq 0 \quad (38)$$

By integrating, we get

$$\ln(V) \geq -\mu t + C_1 \quad (39)$$

$$V \geq e^{-\mu t + C_1} \quad (40)$$

$$V \geq K_1 e^{-\mu t} \quad (41)$$

$$V \geq V(0)e^{-\mu t} \geq 0 \quad (42)$$

Therefore, for all values of t , $V(t)$ is positive. Similarly, the third equation of the model (29) implies that

$$\frac{dE_1}{dt} = \frac{\beta(E_1 + \kappa I_1)}{N} S - (\rho + \mu)E_1 \geq -(\rho + \mu)E_1 \quad \text{or} \quad \frac{dE_1}{dt} \geq -(\rho + \mu)E_1 \quad (43)$$

which can be written as

$$\frac{dE_1}{E_1} \geq -(\rho + \mu)dt, \quad E_1 \neq 0 \quad (44)$$

By integrating, we get

$$\ln(E_1) \geq -(\rho + \mu)t + C_2 \quad (45)$$

$$E_1 \geq e^{-(\rho+\mu)t+C_2} \quad (46)$$

$$E_1 \geq K_2 e^{-(\rho+\mu)t} \quad (47)$$

$$E_1 \geq E_1(0)e^{-(\rho+\mu)t} \geq 0 \quad (48)$$

Therefore, for all values of t , $E_1(t)$ is positive. Similarly, the fourth equation of the model (29) implies that

$$\frac{dE_2}{dt} = \frac{\alpha(E_2 + \psi I_2)}{N} S - (\eta + \mu)E_2 \geq -(\eta + \mu)E_2 \quad \text{or} \quad \frac{dE_2}{dt} \geq -(\eta + \mu)E_2 \quad (49)$$

which can be written as

$$\frac{dE_2}{E_2} \geq -(\eta + \mu)dt, \quad E_2 \neq 0 \quad (50)$$

By integrating, we get

$$\ln(E_2) \geq -(\eta + \mu)t + C_3 \quad (51)$$

$$E_2 \geq e^{-(\eta + \mu)t + C_3} \quad (52)$$

$$E_2 \geq K_3 e^{-(\eta + \mu)t} \quad (53)$$

at $t = 0$,

$$E_2 \geq E_2(0)e^{-(\eta + \mu)t} \geq 0 \quad (54)$$

Therefore, for all values of t , $E_2(t)$ is positive. In the same way, the fifth equation of the model (29) implies that

$$\frac{dI_1}{dt} = \rho E_1 - (\tau + \mu + \delta)I_1 \geq -(\tau + \mu + \delta)I_1 \quad \text{or} \quad \frac{dI_1}{dt} \geq -(\tau + \mu + \delta)I_1 \quad (55)$$

The equation (55) can be written as

$$\frac{dI_1}{I_1} \geq -(\tau + \mu + \delta)dt \quad (56)$$

By integration, we get

$$\ln(I_1) \geq -(\tau + \mu + \delta)t + C_4 \quad (57)$$

$$I_1 \geq e^{-(\tau + \mu + \delta)t + C_4} = K_4 e^{-(\tau + \mu + \delta)t} \quad (58)$$

at $t = 0$,

$$I_1 \geq I_1(0)e^{-(\tau + \mu + \delta)t} \geq 0 \quad (59)$$

Hence, $I(t)$ is also positive in the given interval. In the same way, the sixth equation of the model (29) implies

$$\frac{dI_2}{dt} = \eta E_2 - (\epsilon + \mu + \gamma)I_2 \geq -(\epsilon + \mu + \gamma)I_2 \quad \text{or} \quad \frac{dI_2}{dt} \geq -(\epsilon + \mu + \gamma)I_2 \quad (60)$$

The equation (60) can be written as

$$\frac{dI_2}{I_2} \geq -(\epsilon + \mu + \gamma)dt \quad (61)$$

By integration, we get

$$\ln(I_2) \geq -(\epsilon + \mu + \gamma)t + C_5 \quad (62)$$

$$I_2 \geq e^{-(\epsilon + \mu + \gamma)t + C_5} = K_5 e^{-(\epsilon + \mu + \gamma)t} \quad (63)$$

at $t = 0$,

$$I_2 \geq I_2(0)e^{-(\epsilon + \mu + \gamma)t} \geq 0 \quad (64)$$

Hence, $I_2(t)$ is also positive in the given interval. In the same way, the last equation of the model (29) implies

$$\frac{dR}{dt} = \tau I_1 + \epsilon I_2 - (\mu + \omega)R \geq -(\mu + \omega)R \quad \text{or} \quad \frac{dR}{dt} \geq -(\mu + \omega)R \quad (65)$$

which can be written as

$$\frac{dR}{R} = -(\mu + \omega)dt \quad (66)$$

integrating equation (66), we get

$$\ln(R) = -(\mu + \omega)t + C_6 \quad (67)$$

$$R \geq e^{-(\mu + \omega)t + C_6} = C_6 e^{-(\mu + \omega)t} \quad (68)$$

at $t = 0$

$$R \geq R(0)e^{-(\mu + \omega)t} \geq 0 \quad (69)$$

Hence, it has been proven that $S(t) > 0$, $V(t) > 0$, $E_1(t) > 0$, $E_2(t) > 0$, $I_1(t) > 0$, $I_2(t) > 0$ and $R(t) > 0$ for all $t > 0$.

3.3. The Basic Reproduction Number

Basic reproduction number is a fundamental threshold in mathematical study of epidemiology. It helps to forecast the transmission potential of a disease.

In finding the basic reproduction number associated with model (29), we applied the Next Generation Operator approach where we let \mathcal{F} be the rate of appearance of new infections in the compartments and \mathcal{V} be transition state of the disease classes. In the model (29), we have four disease classes namely: E_1 , E_2 , I_1 , and I_2 .

\mathcal{F} and \mathcal{V} is given by:

$$\mathcal{F} = \begin{bmatrix} \frac{\beta S(E_1 + \kappa I_1)}{N} \\ \frac{\alpha S(E_2 + \psi I_2)}{N} \\ 0 \\ 0 \\ 0 \end{bmatrix}, \text{ and } \mathcal{V} = \begin{bmatrix} \rho E_1 + \mu E_1 \\ \eta E_2 + \mu E_2 \\ \tau I_1 + \mu I_1 + \delta I_1 - \rho E_1 \\ \epsilon I_2 + \mu I_2 + \gamma I_2 - \eta E_2 \end{bmatrix} \quad (70)$$

The derivatives of \mathcal{F} and \mathcal{V} evaluated at the DFE are given by:

$$F = \begin{bmatrix} \frac{\beta(b-\mu-\nu)}{b} & 0 & \frac{\beta(b-\mu-\nu)\kappa}{b} & 0 \\ 0 & \frac{\alpha(b-\mu-\nu)}{b} & 0 & \frac{\alpha(b-\mu-\nu)\psi}{b} \\ 0 & 0 & 0 & 0 \\ 0 & 0 & 0 & 0 \end{bmatrix} \quad (71)$$

and

$$V = \begin{bmatrix} \mu + \rho & 0 & 0 & 0 \\ 0 & \eta + \mu & 0 & 0 \\ -\rho & 0 & \delta + \mu + \tau & 0 \\ 0 & -\eta & 0 & \epsilon + \gamma + \mu \end{bmatrix} \quad (72)$$

respectively. The inverse of V is given by

$$V^{-1} = \begin{bmatrix} \frac{1}{\mu + \rho} & 0 & 0 & 0 \\ 0 & \frac{1}{\eta + \mu} & 0 & 0 \\ \frac{\rho}{(\mu + \rho)(\delta + \mu + \tau)} & 0 & \frac{1}{\delta + \mu + \tau} & 0 \\ 0 & \frac{\eta}{(\eta + \mu)(\epsilon + \gamma + \mu)} & 0 & \frac{1}{(\epsilon + \gamma + \mu)} \end{bmatrix} \quad (73)$$

and calculating the next generation matrix, FV^{-1} , gives

$$FV^{-1} = \begin{bmatrix} a_{11} & 0 & \frac{\beta(b-\mu-\nu)\kappa}{b(\delta + \mu + \tau)} & 0 \\ 0 & a_{22} & 0 & \frac{\alpha(b-\mu-\nu)\psi}{b(\epsilon + \gamma + \mu)} \\ 0 & 0 & 0 & 0 \\ 0 & 0 & 0 & 0 \end{bmatrix} \quad (74)$$

where $a_{11} = \frac{\beta(b-\mu-\nu)}{b(\mu + \rho)} + \frac{\beta(b-\mu-\nu)\kappa\rho}{b(\mu + \rho)(\delta + \mu + \tau)}$, $a_{22} = \frac{\alpha(b-\mu-\nu)}{b(\eta + \mu)} + \frac{\alpha(b-\mu-\nu)\psi\eta}{b(\eta + \mu)(\epsilon + \gamma + \mu)}$

From the Eigenvalues of the next generation matrix, FV^{-1} , the reproduction number R_0 is equal to the spectral radius $\rho(FV^{-1})$, which is also known as the dominant eigenvalue of FV^{-1} , thus $R = \max(R_{0A}, R_{0B})$ where

$$R_{0A} = \frac{\beta(\kappa\rho + \delta + \mu + \tau)(b - \mu - \nu)}{b(\mu + \rho)(\delta + \mu + \tau)}, R_{0B} = \frac{\alpha(b - \mu - \nu)(\eta\psi + \epsilon + \gamma + \mu)}{b(\eta + \mu)(\epsilon + \gamma + \mu)} \quad (75)$$

3.4. Existence of Equilibrium

The equilibrium points related to Model (29) are obtained when the differential equation describing each compartment is at steady state (points where the variables do not change with time). Thus,

$$\begin{cases} \frac{dS}{dt} = bS \left(1 - \frac{S}{N}\right) - \frac{\beta S(E_1 + \kappa I_1)}{N} - \frac{\alpha S(E_2 + \psi I_2)}{N} - \mu S + \omega R - \nu S = 0 \\ \nu S - \mu V = 0 \\ \frac{\beta S(E_1 + \kappa I_1)}{N} - \rho E_1 - \mu E_1 = 0 \\ \frac{\alpha S(E_2 + \psi I_2)}{N} - \eta E_2 - \mu E_2 = 0 \\ \rho E_1 - \tau I_1 - \mu I_1 - \delta I_1 = 0 \\ \eta E_2 - \epsilon I_2 - \mu I_2 - \gamma I_2 = 0 \\ \tau I_1 + \epsilon I_2 - \mu R - \omega R = 0 \end{cases} \quad (76)$$

From the ODE system above (76), we obtained existence of three different equilibria;

1. The Disease Free Equilibrium (DFE)

The disease free equilibrium of the system (76) is given by

$$\xi_0 = (S_0^*, V_0^*, 0, 0, 0, 0, 0) \quad (77)$$

$$\text{where } S_0^* = \frac{N(b - \mu - \nu)}{b} \text{ and } V_0^* = \frac{\nu N(b - \mu - \nu)}{b\mu}$$

2. Boundary equilibrium (BE)

Two boundary equilibrium (BE) points ξ_1 and ξ_2 , are given by

i. In the case where only strain A survives yields

$$\xi_1 = (S_A^*, V_A^*, E_{1A}^*, 0, I_{1A}^*, 0, R_A^*) \quad (78)$$

$$\text{where } S_A^* = \frac{N(b - \mu - \nu)}{bR_{0A}}, \quad V_A^* = \frac{\nu N(b - \mu - \nu)}{b\mu R_{0A}}, \quad E_{1A}^* = \frac{L_1(R_{0A} - 1)}{D_1}, \quad I_{1A}^* = \frac{\rho E_{1A}^*}{(\delta + \mu + \tau)} \text{ and } R_A^* = \frac{\rho \tau E_{1A}^*}{(\delta + \mu + \tau)(\mu + \omega)}$$

ii. In the case where only strain B survives yields

$$\xi_2 = (S_B^*, V_B^*, 0, E_{2B}^*, 0, I_{2B}^*, R_B^*) \quad (79)$$

$$\text{where } S_B^* = \frac{N(b - \mu - \nu)}{bR_{0B}}, \quad V_B^* = \frac{\nu N(b - \mu - \nu)}{b\mu R_{0B}}, \quad E_{2B}^* = \frac{L_2(R_{0B} - 1)}{D_2}, \quad I_{2B}^* = \frac{\eta E_{2B}^*}{(\epsilon + \gamma + \mu)} \text{ and } R_B^* = \frac{\eta \epsilon E_{2B}^*}{(\epsilon + \gamma + \mu)(\mu + \omega)}$$

where

$$L_1 = N(\mu + \rho)(\delta + \mu + \tau)^2 b(\mu + \rho)(\delta + \mu + \tau)(\mu + \omega),$$

$$L_2 = N(\eta + \mu)(\epsilon + \gamma + \mu)^2 b(\eta + \mu)(\epsilon + \gamma + \mu)(\mu + \omega),$$

$$D_1 = \beta^2(\kappa\rho + \delta + \mu + \tau)^2(\delta\mu^2 + \delta\mu\omega + \delta\mu\rho + \delta\omega\rho + \mu^3 + \mu^2\omega + \mu^2\rho + \mu^2\tau + \mu\omega\rho + \mu\omega\tau + \mu\rho\tau), \quad \text{and}$$

$$D_2 = \alpha^2(\eta\psi + \epsilon + \gamma + \mu)^2(\epsilon\eta\mu + \epsilon\mu^2 + \epsilon\mu\omega + \eta\gamma\mu + \eta\gamma\omega + \eta\mu^2 + \eta\mu\omega + \gamma\mu^2 + \gamma\mu\omega + \mu^3 + \mu^2\omega)$$

3.5. Local Stability Analysis of the Disease Free-Equilibrium

Theorem 3.2. The disease-free equilibrium ξ_0 is unstable if $R_0 > 1$ while it is locally asymptotically stable if $R_0 < 1$ [20].

Proof: To prove the local stability of the equilibrium points of the model, the corollary of Gershgorin circle theorem is employed.

Corollary 2.1: (Corollary of Gershgorin Circle Theorem) Let A be an $n \times n$ matrix with real entries. If the diagonal elements

a_{ii} of A satisfy

$$a_{ii} < -r_i \quad (80)$$

where

$$r_i = \sum_{j=1, j \neq i}^n |a_{ij}| \quad (81)$$

for $i = 1, \dots, n$, then the eigenvalues of A are negative or have negative real parts [20].

The Jacobian matrix associated with the model system 29 evaluated at the disease-free equilibrium is given by:

$$J_{dfe} = J(\xi_0) = \begin{bmatrix} a_{11} & 0 & a_{13} & a_{14} & a_{15} & a_{16} & \omega \\ \nu & -\mu & 0 & 0 & 0 & 0 & 0 \\ 0 & 0 & a_{33} & 0 & a_{35} & 0 & 0 \\ 0 & 0 & 0 & a_{44} & 0 & a_{46} & 0 \\ 0 & 0 & \rho & 0 & a_{55} & 0 & 0 \\ 0 & 0 & 0 & \eta & 0 & a_{66} & 0 \\ 0 & 0 & 0 & 0 & \tau & \epsilon & a_{77} \end{bmatrix} \quad (82)$$

where $a_{11} = b \left(1 - \frac{(b - \mu - \nu)}{b}\right) - b$, $a_{13} = -\frac{\beta(b - \mu - \nu)}{b}$, $a_{14} = -\frac{\alpha(b - \mu - \nu)}{b}$, $a_{15} = -\frac{\beta(b - \mu - \nu)\kappa}{b}$, $a_{16} = -\frac{\alpha(b - \mu - \nu)\psi}{b}$, $a_{33} = \frac{\beta(b - \mu - \nu)}{b} - \rho - \mu$, $a_{35} = \frac{\beta(b - \mu - \nu)\kappa}{b}$, $a_{44} = \frac{\alpha(b - \mu - \nu)}{b} - \eta - \mu$, $a_{46} = \frac{\alpha(b - \mu - \nu)\psi}{b}$, $a_{55} = -\delta - \mu - \tau$, $a_{66} = -\epsilon - \gamma - \mu$, $a_{77} = -\mu - \omega$

From column 2 the matrix of (82), we get eigenvalue $\lambda_1 = -\mu$ which is negative. Eliminating row 2 and column 2 from the matrix (82), we end up with the sub-matrix

$$J = \begin{bmatrix} a_{11} & a_{13} & a_{14} & a_{15} & a_{16} & \omega \\ 0 & a_{33} & 0 & a_{35} & 0 & 0 \\ 0 & 0 & a_{44} & 0 & a_{46} & 0 \\ 0 & \rho & 0 & a_{55} & 0 & 0 \\ 0 & 0 & \eta & 0 & a_{66} & 0 \\ 0 & 0 & 0 & \tau & \epsilon & a_{77} \end{bmatrix} \quad (83)$$

From column 1 the matrix of (83), we get eigenvalue $\lambda_1 = a_{11} = -b + \mu + \nu$ which is negative. Eliminating row 1 and column 1 from the matrix (83), we end up with the sub-matrix

$$J = \begin{bmatrix} a_{33} & 0 & a_{35} & 0 & 0 \\ 0 & a_{44} & 0 & a_{46} & 0 \\ \rho & 0 & a_{55} & 0 & 0 \\ 0 & \eta & 0 & a_{66} & 0 \\ 0 & 0 & \tau & \epsilon & a_{77} \end{bmatrix} \quad (84)$$

From last column the matrix of (84), we get eigenvalue $\lambda_1 = a_{77} = -\mu - \omega$ which is negative. Eliminating the last row and column from the matrix (84), we end up with the sub-matrix

$$J = \begin{bmatrix} a_{33} & 0 & a_{35} & 0 \\ 0 & a_{44} & 0 & a_{46} \\ \rho & 0 & a_{55} & 0 \\ 0 & \eta & 0 & a_{66} \end{bmatrix} \quad (85)$$

The matrix 85 satisfies the corollary of Gershgorin's circle theorem, if the following inequalities hold;

$$\begin{cases} a_{33} < -a_{35} & \Rightarrow & b(\mu + \rho) > \beta(b - \mu - \nu)(\kappa + 1) \\ a_{44} < -a_{46} & \Rightarrow & b(\eta + \mu) > \alpha(b - \mu - \nu)(\psi + 1) \\ a_{55} < -\rho & \Rightarrow & \delta + \mu + \tau > \rho \\ a_{66} < -\eta & \Rightarrow & \epsilon + \gamma + \mu > \eta \end{cases} \quad (86)$$

Multiplying and simplifying the first and third equation of (86) gives

$$1 > \frac{\beta(b - \mu - \nu)(\kappa + 1)\rho}{b(\mu + \rho)(\delta + \mu + \tau)} \quad (87)$$

which can be expressed as

$$1 > \Lambda_A R_{0A} \quad (88)$$

$$\text{where } \Lambda_A = \frac{(\kappa + 1)\rho}{\kappa\rho + \delta + \mu + \tau}$$

For equation (88) to hold, $R_{0A} < 1$.

Similarly, multiplying and simplifying the second and last equation of (86) gives

$$1 > \frac{\alpha(b - \mu - \nu)(\psi + 1)\eta}{b(\eta + \rho)(\epsilon + \gamma + \mu)} \quad (89)$$

which can be also be expressed as

$$1 > \Lambda_B R_{0B} \quad (90)$$

$$\text{where } \Lambda_B = \frac{(\psi + 1)\eta}{\eta\psi + \epsilon + \gamma + \mu}$$

For equation (90) to hold, $R_{0B} < 1$.

Therefore, $R_{0A} < 1$ and $R_{0B} < 1$, ensures local stability of the disease free equilibrium.

3.6. Local Stability Analysis of the Strain A Boundary Equilibrium

Theorem 4.3 Strain A equilibrium point $\xi_1 = (S^*, V^*, E_1^*, 0, I_1^*, 0, R^*)$ is locally asymptotically stable if and only if $R_{0A} > 1$.

Proof

The Jacobian matrix evaluated at ξ_1 is given as

$$J(\xi_1) = \begin{bmatrix} A_{11} & 0 & A_{13} & A_{14} & A_{15} & A_{16} & \omega \\ \nu & -\mu & 0 & 0 & 0 & 0 & 0 \\ A_{31} & 0 & A_{33} & 0 & A_{35} & 0 & 0 \\ 0 & 0 & 0 & A_{44} & 0 & A_{46} & 0 \\ 0 & 0 & \rho & 0 & A_{55} & 0 & 0 \\ 0 & 0 & 0 & \eta & 0 & A_{66} & 0 \\ 0 & 0 & 0 & 0 & \tau & \epsilon & A_{77} \end{bmatrix} \quad (91)$$

$$\text{where } A_{11} = b - \frac{t_1}{R_{0A}N} - \frac{\beta(R_{0A} - 1)(\kappa t_4 + t_3)}{N} - \mu - \nu, A_{13} = -\frac{\beta t_1}{R_{0A}N}, A_{14} = -\frac{\alpha t_1}{R_{0A}N}, A_{15} = -\frac{\beta t_1 \kappa}{R_{0A}N}, A_{16} = -\frac{\alpha t_1 \psi}{R_{0A}N}, A_{33} = \frac{\beta t_1}{R_{0A}N} - \rho - \mu, A_{35} = \frac{\beta t_1 \kappa}{R_{0A}N}, A_{44} = \frac{\alpha t_1}{R_{0A}N} - \eta - \mu, A_{46} = \frac{\alpha t_1 \psi}{R_{0A}N}, A_{55} = -\delta - \mu - \tau, A_{66} = -\epsilon - \gamma - \mu, A_{77} = -\mu - \omega, t_1 = \frac{N(b - \mu - \nu)}{b}, t_2 = \frac{\nu N(b - \mu - \nu)}{b\mu}, t_3 = \frac{L_1}{D_1}, t_4 = \frac{\rho L_1}{D_1(\delta + \mu + \nu)} \text{ and } t_5 = \frac{\rho \tau L_1}{D_1(\delta + \mu + \tau)(\mu + \omega)}$$

From second column the matrix of 91, we get eigenvalue $\lambda_1 = -\mu$ which is negative. Eliminating the second row and column from the matrix (91) yields

$$J_{\xi_1} = \begin{bmatrix} A_{11} & A_{13} & A_{14} & A_{15} & A_{16} & \omega \\ A_{31} & A_{33} & 0 & A_{35} & 0 & 0 \\ 0 & 0 & A_{44} & 0 & A_{46} & 0 \\ 0 & \rho & 0 & A_{55} & 0 & 0 \\ 0 & 0 & \eta & 0 & A_{66} & 0 \\ 0 & 0 & 0 & \tau & \epsilon & A_{77} \end{bmatrix} \quad (92)$$

Using the corollary of Gershgorin's circle theorem (Corollary 4.1), the matrix 92 will have negative eigenvalues if the following inequalities are satisfied. That is,

$$\begin{cases} A_{11} < -(A_{13} + A_{14} + A_{15} + A_{16} + \omega) \\ A_{33} < -(A_{31} + A_{35}) \\ A_{44} < -A_{46} \\ A_{55} < -\rho \\ A_{66} < -\eta \\ A_{77} < -(\tau + \epsilon) \end{cases} \quad (93)$$

Considering the first equation of 93 gives

$$b - \frac{2bt_1}{R_{0A}N} - \frac{\beta(R_{0A} - 1)(\kappa t_4 + t_3)}{N} - \mu - \nu < -\frac{(\alpha(\psi + 1) + \beta(\kappa + 1))t_1}{R_{0A}N} - \omega \quad (94)$$

Simplifying (94) above yields

$$\frac{\beta(R_{0A} - 1)(\kappa t_4 + t_3)}{N} + \frac{2bt_1}{R_{0A}N} + \mu + \nu - b > \frac{(\alpha(\psi + 1) + \beta(\kappa + 1))t_1}{R_{0A}N} + \omega \quad (95)$$

Also, considering the second equation of (93) and simplifying gives

$$\frac{\beta t_1(\kappa + 1)}{R_{0A}N} < -\frac{\beta(R_{0A} - 1)(\kappa t_4 + t_3)}{N} + \rho + \mu \quad (96)$$

Similarly, considering the third equation of (93) and simplifying gives

$$\frac{\alpha t_1(\psi + 1)}{R_{0A}N} < \eta + \mu \quad (97)$$

Adding equation (96) and (97) gives

$$\frac{(\alpha(\psi + 1) + \beta(\kappa + 1))t_1}{R_{0A}N} < -\frac{\beta(R_{0A} - 1)(\kappa t_4 + t_3)}{N} + \rho + \eta + 2\mu \quad (98)$$

Substituting equation (98) in equation (95) and simplifying

$$\frac{2\beta(R_{0A} - 1)(\kappa t_4 + t_3)}{N} + \frac{2bt_1}{R_{0A}N} + \nu > \rho + \eta + \mu + b \quad (99)$$

For the above inequality to hold $(R_{0A} - 1) > 0$ which implies that $R_{0A} > 1$

Therefore, $R_{0A} > 1$, ensures local stability of the endemic equilibrium for the strain A .

3.7. Local Stability Analysis of the Strain B Boundary Equilibrium

Theorem 4.4 Strain B equilibrium point $\xi_2 = (S^*, V^*, 0, E_2^*, 0, I_2^*, R^*)$ is locally asymptotically stable if and only if $R_{0B} > 1$.

Proof

The Jacobian matrix evaluated at ξ_2 is given as

$$J(\xi_2) = \begin{bmatrix} B_{11} & 0 & B_{13} & B_{14} & B_{15} & B_{16} & \omega \\ \nu & -\mu & 0 & 0 & 0 & 0 & 0 \\ 0 & 0 & B_{33} & 0 & B_{35} & 0 & 0 \\ B_{41} & 0 & 0 & B_{44} & 0 & B_{46} & 0 \\ 0 & 0 & \rho & 0 & B_{55} & 0 & 0 \\ 0 & 0 & 0 & \eta & 0 & B_{66} & 0 \\ 0 & 0 & 0 & 0 & \tau & \epsilon & B_{77} \end{bmatrix} \quad (100)$$

where $B_{11} = b - \frac{2bd_1}{R_{0B}N} - \frac{\beta(R_{0B} - 1)(\psi d_4 + d_3)}{N} - \mu - \nu$, $B_{13} = -\frac{\beta d_1}{R_{0B}N}$, $B_{14} = -\frac{\alpha d_1}{R_{0B}N}$, $B_{15} = -\frac{\beta d_1 \kappa}{R_{0B}N}$, $B_{16} = -\frac{\alpha d_1 \psi}{R_{0B}N}$, $B_{33} = \frac{\beta d_1}{R_{0B}N} - \rho - \mu$, $B_{35} = \frac{\beta d_1 \kappa}{RN}$, $B_{44} = \frac{\alpha d_1}{RN} - \eta - \mu$, $B_{46} = \frac{\alpha t_1 \psi}{R_{0B}N}$, $B_{55} = -\delta - \mu - \tau$, $B_{66} = -\epsilon - \gamma - \mu$,

$$B_{77} = -\mu - \omega, d_1 = \frac{N(b - \mu - \nu)}{b}, d_2 = \frac{\nu N(b - \mu - \nu)}{b\mu}, d_3 = \frac{L_2}{D_2}, d_4 = \frac{\rho L_2}{D_3(\epsilon + \gamma + \mu)} \text{ and } d_5 = \frac{\rho \tau L_2}{D_2(\epsilon + \gamma + \mu)(\mu + \omega)}$$

From second column the matrix of (100), we get eigenvalue $\lambda_1 = -\mu$ which is negative. Eliminating the second row and column from the matrix (100) yields

$$J(\xi_2) = \begin{bmatrix} B_{11} & B_{13} & B_{14} & B_{15} & B_{16} & \omega \\ 0 & B_{33} & 0 & A_{35} & 0 & 0 \\ B_{41} & 0 & B_{44} & 0 & B_{46} & 0 \\ 0 & \rho & 0 & B_{55} & 0 & 0 \\ 0 & 0 & \eta & 0 & B_{66} & 0 \\ 0 & 0 & 0 & \tau & \epsilon & B_{77} \end{bmatrix} \quad (101)$$

Similarly, using the corollary of Gershgorin's circle theorem (Corollary 4.1), the matrix 101 will have negative eigenvalues if the following inequalities are satisfied. That is,

$$\begin{cases} B_{11} < -(B_{13} + B_{14} + B_{15} + B_{16} + \omega) \\ B_{33} < -B_{35} \\ B_{44} < -(B_{41} + B_{46}) \\ B_{55} < -\rho \\ B_{66} < -\eta \\ B_{77} < -(\tau + \epsilon) \end{cases} \quad (102)$$

Considering the first equation of 102 gives

$$b - \frac{2bd_1}{NR_{0B}} - \frac{\alpha(R_{0B} - 1)(\psi d_4 + d_3)}{N} - \mu - \nu < -\frac{(\alpha(\psi + 1) + \beta(\kappa + 1))d_1}{NR_{0B}} - \omega \quad (103)$$

Simplifying equation (103) above yields

$$\frac{\alpha(R_{0B} - 1)(\psi d_4 + d_3)}{N} + \frac{2bd_1}{NR_{0B}} + \mu + \nu - b > \frac{(\alpha(\psi + 1) + \beta(\kappa + 1))d_1}{NR_{0B}} + \omega \quad (104)$$

Also, considering the second equation of (102) and simplifying gives

$$\frac{\beta d_1(\kappa + 1)}{NR_{0B}} < \rho + \mu \quad (105)$$

Similarly, considering the third equation of (102) and simplifying gives

$$\frac{\alpha d_1(\psi + 1)}{NR_{0B}} < -\frac{\alpha(R_{0B} - 1)(\psi d_4 + d_3)}{N} + \rho + \mu \quad (106)$$

Adding equation (105) and (106) gives

$$\frac{(\alpha(\psi + 1) + \beta(\kappa + 1))d_1}{NR_{0B}} < -\frac{\alpha(R_{0B} - 1)(\psi d_4 + d_3)}{N} + \rho + \eta + 2\mu \quad (107)$$

Substituting equation (107) in equation (104) and simplifying

$$\frac{2\alpha(R_{0B} - 1)(\psi d_4 + d_3)}{N} + \frac{2bd_1}{NR_{0B}} + \nu > \rho + \eta + \mu + b + \omega \quad (108)$$

In the same way, for the above inequality to hold $(R_{0B} - 1) > 0$ which implies that $R_{0B} > 1$.

Therefore, $R_{0B} > 1$, ensures local stability of the endemic equilibrium for the strain B .

3.8. Numerical Simulation

In this subsection, an illustration of the numerical results in this work is given by carrying out numerical simulations of the

model system. The parameters used in the simulation of the model were taken from various sources and some also were estimated based on data from World Health Organisation. All simulations in this section were performed using the MAPLE Software. The table below defines the value of the parameters used in the simulations and the sources from which these values were obtained.

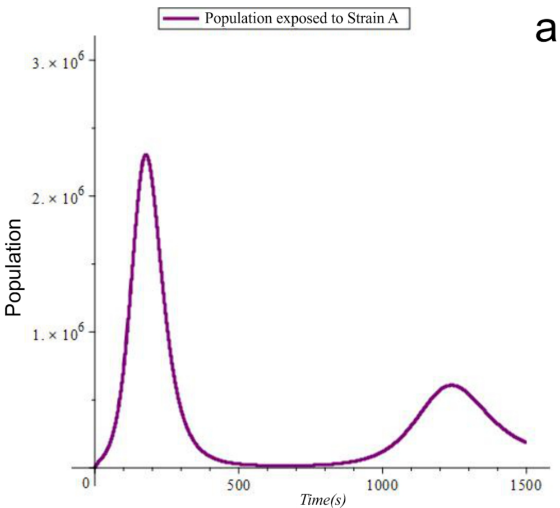


Figure 6. The Disease Classes.

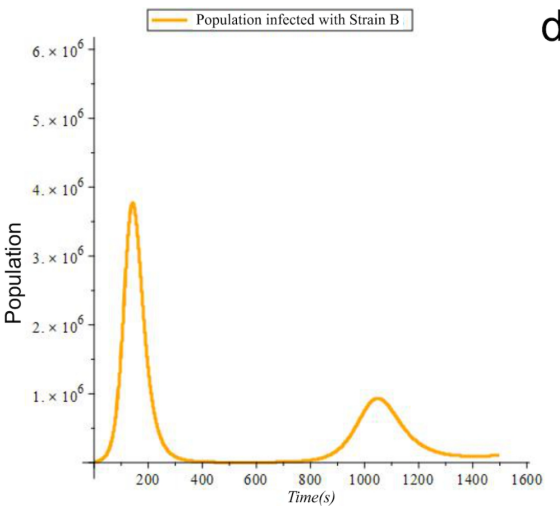


Figure 9. The Disease Classes.

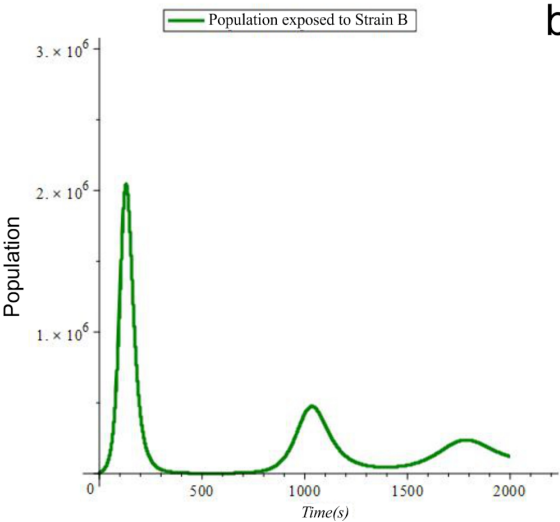


Figure 7. The Disease Classes.

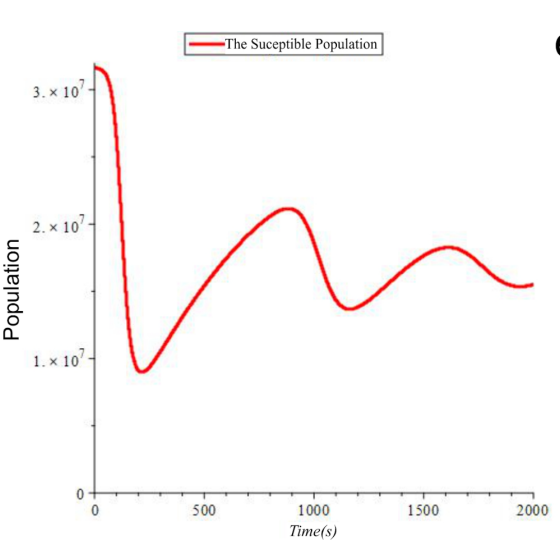


Figure 10. Non Disease Classes.

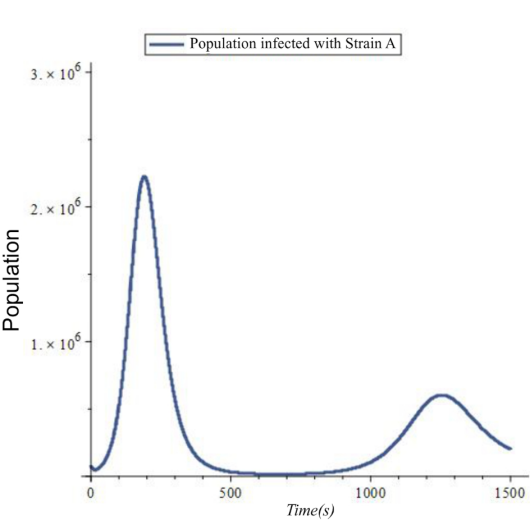


Figure 8. The Disease Classes.

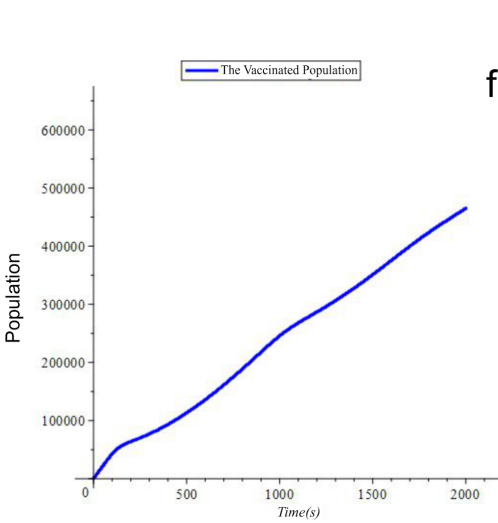


Figure 11. Non Disease Classes.

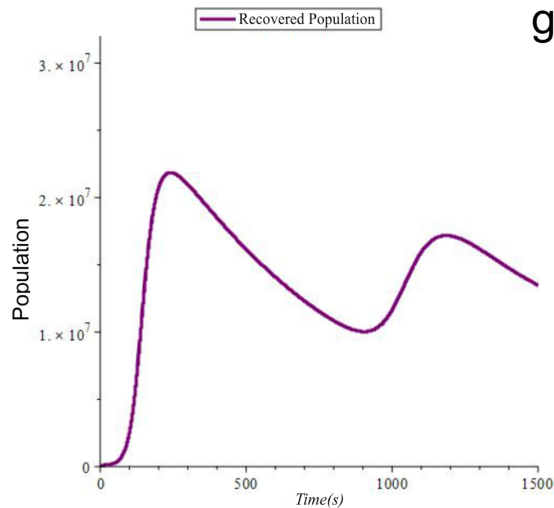


Figure 12. Non Disease Classes.

Table 3. Parameters and Sources of Values Used.

Symbol	Value	Source
N	32,000,000	WHO (2021)
b	0.000079452	Estimated
ν	0.000014	Estimated
μ	0.000019726	Estimated
β	0.021829	Estimated
α	0.091829	Estimated
ρ	1/14	Estimated
η	1/7	Estimated
τ	0.07143	Estimated
δ	0.000017992	Estimated
ε	0.07143	Estimated
γ	0.000027992	Estimated
ω	1/730	Estimated
κ	1	Estimated
ψ	1	Estimated

4. Discussion

When the infection is first introduced into the population, a significant number of individuals become exposed to the disease. This rapid exposure causes a sharp decrease in the susceptible population as these individuals move to the exposed class. In figure 10, when the infection is first introduced into the population, a significant number of individuals become exposed to the disease. This rapid exposure causes a sharp decrease in the susceptible population as these individuals move to the exposed class. While the susceptible population is decreasing, the exposed population increases. This is because individuals who were initially susceptible are now becoming exposed to the infection. This dynamic is depicted in Figure 6.

As coupled with treatment and other measures to curtail the spread of the disease, there is a downward trend in the exposed

class as seen in Figures 6 and 7. This same phenomenon can be explained for that of the infectious class. As the disease is ravaging the population, it is seen that the exposed class increase and this leads to the infected class experience an initial increase as seen in Figures 8 and 9. Individuals and government try to put in measures to control the disease. As that continues, the number of the exposed class will fall and in the same way, the number of the infectious population will also fall. It will fall to the point until individuals relax with the measures put in place to combat the disease. As individuals relax in their effort to follow the protocols, there is an increase again. This phenomenon will continue but each increase will not be as of the first and it further continues until the disease eventually almost dies out.

In the absence of one strain, for example, in the absence of strain B, Figures 6 and 8 are the behavior of strain A. When a new strain (strain B) with higher transmissibility is introduced into the system, it quickly overshadows the existing strain (strain A). The strain with higher transmissibility has a greater basic reproduction number (R_0), allowing it to spread more rapidly and outcompete the strain with lower transmissibility.

In our simulation, we had R_0 to be 0.9957945674 for strain A and 1.109170840 for strain B.

5. Conclusion

The study successfully formulated and analyzed a two-strain compartmental (Susceptible, Vaccination, Infected and Recovered) model of SARS-CoV-2, highlighting the dynamic between two different viral strains in a population. Findings from the analysis of the model showed that there were three equilibrium points: the diseases-free equilibrium (DFE) and boundary equilibrium for strain A (EEA) and strain B (EEB). At the Disease-Free Equilibrium (DFE), no individuals in the population are infected with either strain of the virus. It indicates the absence of the disease, with all individuals remaining susceptible. At EEA, strain A persists in the population while strain B is absent and at EEB, strain B persist in the population while strain A is not.

The findings emphasize the critical role of the basic reproduction number (R_0) in determining the stability and spread of the virus. Statainability analysis of the model showed that when (R_0) is less than unity at the Disease-Free Equilibrium, the infection will eventually die out, while a value greater than unity at the Boundary Equilibriums signifies sustained transmission.

Simulation results highlighted the necessity for enhanced vaccination efforts to achieve herd immunity and control the spread of the virus. In addition to vaccination, the study recommends implementing comprehensive control measures, including face masks, social distancing, and contact tracing, to mitigate the spread of SARS-CoV-2. Implementing these recommendations will be crucial in managing the pandemic and safeguarding public health.

ORCID

0009-0007-5980-1303 (John Cobbinah)
 0009-0007-8513-6992 (Samuella Boadi)
 0000-0003-2948-681X (Monica Veronica Crankson)

Conflicts of Interest

The authors declare no conflicts of interest.

References

- [1] Danso-Addo, E., Boadi, S., Cobbinah, J. A Mathematical Model of the Transmission of COVID-19 in Ghana. *American Journal of Applied Mathematics*. 2023, 11(6), 119-129. <https://doi.org/10.11648/j.ajam.20231106.13>
- [2] Jebiril, N. World Health Organization declared a pandemic public health menace: a systematic review of the coronavirus disease 2019 COVID-19. 2020, Vol. 1, No. 2, pp. 1-5. <https://doi.org/10.2139/ssrn.3563992>
- [3] World Health Organisation. “World Health Organisation (WHO) Coronavirus (COVID-19) Dashboard”. Available from: <https://covid19.who.int/> [Accessed: August 1, 2021].
- [4] World Health Organisation. “World Health Organisation (WHO) Coronavirus (COVID-19) Dashboard-Ghana”. Available from: <https://covid19.who.int/region/afro/country/gh> [Accessed: August 1, 2021]
- [5] Halim, M. A Report on COVID-19 Variants, COVID-19 Vaccines and the Impact of the Variants on the Efficacy of the Vaccines. *J Clin Med Res*. 2021, Vol. 3, No. 2, pp. 1-19. <https://doi.org/10.31254/jcmr.2021.0302>
- [6] Duong, D. Alpha, Beta, Delta, Gamma: What’s Important to Know About SARS-CoV-2 Variants of Concern. 2021, pp. 2-8. <https://doi.org/10.1503/cmaj.1095949>
- [7] Torjesen, I. Covid-19: Delta Variant is Now UK’s Most Dominant Strain and Spreading Through Schools. 2021, 23 pp. <https://doi.org/10.1136/bmj.n1445>
- [8] Agoti, C. N., Ochola-Oyier, L. I., Mohammed, K. S., Lambisia, A. W., de Laurent, Z. R., Morobe, J. M., Mburu, M. W., Omuoyo, D. O., Ongera, E. M., Ndwiga, L. Genomic Surveillance Reveals the Spread Patterns of SARS-CoV-2 in Coastal Kenya During the First Two Waves. *medRxiv*. 2021, 12 pp. <https://doi.org/10.1101/2021.07.06.21260162>
- [9] Khyar, O. and Allali, K. Global Dynamics of a Multi-Strain SEIR Epidemic Model with General Incidence Rates: Application to COVID-19 Pandemic, *Nonlinear Dynamics*. 2020, Vol. 102, No. 1, pp. 489-509. <https://doi.org/10.1007/s11071-020-05929-4>
- [10] Fudolig, M. and Howard, R. The Local Stability of a Modified Multi-Strain SIR Model for Emerging Viral Strains. *PloS one*. 2020, Vol. 15, No. 12, pp. e24-e34.
- [11] Arruda, E. F., Pastore, D. H., Dias, C. M., and Das, S. S. Modeling and Optimal Control of Multi Strain Epidemics, with Application to COVID-19. 2021, pp. 2-6. <https://doi.org/10.1371/journal.pone.0243408>
- [12] Zill, D. G. A First Course in Differential Equations with Modeling Applications. *Cengage Learning*. 2012, 34 pp
- [13] Tolles, J. and Luong, T. Modeling Epidemics with Compartmental Models. *Jama*. 2020, Vol. 323, No. 24, pp. 2515-2516. <https://doi.org/10.1001/jama.2020.8420>
- [14] Sutton, K. M. Discretizing the SI Epidemic Model. *Rose-Hulman Undergraduate Mathematics Journal*. 2014, Vol. 15, No. 1, 12 pp.
- [15] Delamater, P. L., Street, E. J., Leslie, T. F., Yang, Y. T., and Jacobsen, K. H. Complexity of the Basic Reproduction Number. *Emerging infectious diseases*. 2019, Vol. 25, No. 1, pp. 1-3. <https://doi.org/10.3201/eid2501.171901>
- [16] Anastassopoulou, C., Russo, L., Tsakris, A., and one, S. Data-Based Analysis, Modeling and Forecasting of the COVID-19 Outbreak. 2020, Vol. 15, No. 3, pp. e02 -e04. <https://doi.org/10.1371/journal.pone.0230405>
- [17] Ma, Z. Dynamical Modeling and Analysis of Epidemics *World Scientific*. 2009, pp. 2-23.
- [18] Diekmann, O.; Heesterbeek, J. A. P.; Metz, J. A. J. On the definition and the computation of the basic reproduction ratio R_0 in models for infectious diseases in heterogeneous populations. *Journal of Mathematical Biology*. (1990-8-4), 365-382. <https://doi.org/10.1007/BF00178324>
- [19] Wu, S., Tian, C., Liu, P., Guo, D., Zheng, W., Huang, X., Zhang, Y., and Liu, L. Effects of SARS-CoV-2 Mutations on Protein Structures and Intraviral Protein? Protein Interactions. *Journal of medical virology*. 2021, Vol. 93, No. 4, pp. 2132-2140. <https://doi.org/10.1002/jmv.26597>
- [20] Zhang, Z., Zeb, A., Alzahrani, E., and Iqbal, S. Crowding effects on the dynamics of COVID-19 mathematical model. *Advances in Difference Equations*. 2020, No. 1, pp. 1-13. <https://doi.org/10.1186/s13662-020-03137-3>